Optimal Stencils in Sobolev Spaces

Oleg Davydov[1] and Robert Schaback[2]

Draft of November 16, 2016

Abstract: This paper proves that the approximation of pointwise derivatives of order s of functions in Sobolev space $W_2^m(\mathbb{R}^d)$ by linear combinations of function values cannot have a convergence rate better than $m-s-d/2$, no matter how many nodes are used for approximation and where they are placed. These convergence rates are attained by *scalable* approximations that are exact on polynomials of order at least $\lfloor m-d/2\rfloor+1$, proving that the rates are optimal for given m, s, and d. And, for a fixed node set $X\subset\mathbb{R}^d$, the convergence rate in any Sobolev space $W_2^m(\Omega)$ cannot be better than $q-s$ where q is the maximal possible order of polynomial exactness of approximations based on X, no matter how large m is. In particular, scalable stencil constructions via polyharmonic kernels are shown to realize the optimal convergence rates, and good approximations of their error in Sobolev space can be calculated via their error in Beppo-Levi spaces. This allows to construct near-optimal stencils in Sobolev spaces stably and efficiently, for use in meshless methods to solve partial differential equations via generalized finite differences (RBF-FD). Numerical examples are included for illustration.

arXiv:1611.04750v1 [math.NA] 15 Nov 2016

1 Introduction

We consider discretizations of continuous linear functionals $\lambda : U\to\mathbb{R}$ on some normed linear space U of real-valued functions on some bounded domain $\Omega\subset\mathbb{R}^d$. The discretizations are *nodal*, i.e. they work with values $u(x_j)$ of functions $u\in U$ on a set $X=\{x_1,\ldots,x_M\}\subset\Omega$ of *nodes* by

$$\lambda(u)\approx\lambda_{a,X}(u):=\sum_{j=1}^{M}a_j u(x_j)\text{ for all }u\in U. \tag{1}$$

The background is that most operator equations can be written as infinitely may linear equations

$$\lambda(u)=f_\lambda\text{ for all }\lambda\in\Lambda\subset U^*,$$

where the functionals evaluate weak or strong derivatives or differential operators like the Laplacian or take boundary values. This means that the classical approach

[1]Univ. Gießen, Oleg.Davydov@math.uni-giessen.de
https://www.staff.uni-giessen.de/odavydov/

[2]Univ. Göttingen, schaback@math.uni-goettingen.de
http://num.math.uni-goettingen.de/schaback/research/group.html

of *meshless methods* is taken, namely to write the approximations *entirely in terms of nodes* [6].

Our concern is to find *optimal* approximations in Sobolev space $W_2^m(\Omega)$ for domains $\Omega \subset \mathbb{R}^d$. Their calculation is computationally costly and very unstable, but we shall prove that there are *suboptimal* approximations that can be calculated cheaply and stably, namely via *scalable* approximations that have a certain exactness on polynomials (Section 4) and may be constructed via polyharmonic kernels (Section 5). In particular, we shall show that they can have the same convergence rate as the optimal approximations, and we present the minimal assumptions on the node sets to reach that optimal rate.

The application for all of this is that error bounds and convergence rates for nodal approximations to linear functionals enter into the consistency part of the error analysis [30] of nodal meshless methods. These occur in many papers in Science and Engineering, e.g. [1, 2, 4, 8, 15, 14, 16, 17, 18, 22, 26, 32, 33, 34, 35, 36, 37, 38, 41, 42], and several authors have analyzed the construction of nodal approximations mathematically, e.g. [9, 10, 11, 19, 20, 24, 40], but without considering optimal convergence rates.

To get started, we present a suitable notion of *scalability* in Section 2 that allows to define error functionals $\varepsilon_h \in U^*$ based on the scaled point set hX for small $h > 0$ and to prove *convergence rates* k in the sense that error bounds of the form $\|\varepsilon_h\|_{U^*} \le Ch^k$ hold for $h \to 0$. The standard *derivative order* $|\alpha|$ of a pointwise multivariate derivative functional $\lambda(u) := D^\alpha u(0)$ will reappear as a *scaling* order $s(\lambda)$ that governs how the approximations of a functional λ scale for $h \to 0$.

Of course, optimal error bounds will crucially depend on the space U and the node set X. If U contains all real-valued polynomials, the achievable convergence rate of an approximation of a functional λ based on a node set X is limited by the maximal convergence rate on the subspace of polynomials. Section 3 will prove that the upper limit of the convergence rate on polynomials is $q_{max}(\lambda, X) - s(\lambda)$ where q_{max} is the maximal order of polynomials on which the approximation is exact, and that this rate can be reached by *scalable* approximations constructed via exactness on polynomials.

But even if the node set X is large enough to let approximations be exact on high-order polynomials, the convergence rate may be restricted by limited smoothness of the functions in U. In Sobolev spaces $W_2^m(\mathbb{R}^d)$ or $W_2^m(\Omega)$ with $\Omega \subset \mathbb{R}^d$ the achievable rate for arbitrarily large node sets X turns out to be bounded above by $m - d/2 - s(\lambda)$ in Section 4, so that

$$\min\left(m - d/2 - s(\lambda), q_{max}(\lambda, X) - s(\lambda)\right), \tag{2}$$

is a general formula for an upper bound on the convergence rate in Sobolev space $W_2^m(\mathbb{R}^d)$, and this is confirmed by numerical experiments in Section 8.

Then Sections 3, 4, and 5 prove that the convergence rate (2) is *optimal*, and it can be achieved by *scalable* stencils based solely on exactness on polynomials. Furthermore, Section 7 gives a sufficient condition for the convergence of optimal stencils to scalable stencils.

A particularly interesting case is the *best compromise* case where the two constraints on the convergence rate are equal, i.e.

$$q_{max}(\lambda, X) = \lceil m - d/2 \rceil. \tag{3}$$

For a given smoothness m it yields the sparsest approximation that has the optimal convergence rate (or comes arbitrarily close to it if $m-d/2$ is an integer), and for a given sparsity via X it provides the minimal smoothness that is required to realize the maximal possible rate of convergence using that node set.

The numerical examples are collected in Section 8, while the final section 9 summarizes our results and points out a few open problems for further research.

2 Scalability

We now study the behavior of functionals and their approximations under *scaling*.

Definition 1. *1. A domain $\Omega \subset \mathbb{R}^d$ is* scalable, *if it contains the origin as an interior point and satisfies $h\Omega \subseteq \Omega$ for all $0 \le h \le 1$, i.e. if Ω is star–shaped with repect to the origin.*

2. A space U of functions on a scalable domain Ω is scalable, *if $u(h\cdot)$ is in U for all $0 < h \le 1$ and all $u \in U$.*

3. A functional $\lambda \in U^*$ on a scalable space U has scaling order *or* homogeneity order *s if*

$$\lambda(u(h\cdot)) = h^s \lambda(u) \text{ for all } u \in U.$$

Of course, this means that the functional λ must be local in or near the origin. For example, the standard strong functionals are modelled by multivariate derivatives

$$\lambda_\alpha(u) = \frac{\partial^\alpha u}{\partial x^\alpha}(0)$$

at zero, with the scaling behaviour

$$\lambda_\alpha(u(h\cdot)) \quad = \quad h^{|\alpha|}\lambda_\alpha(u)$$

showing that the scaling order coincides with the order of differentiation here. This generalizes to all linear homogeneous differential operators, e.g. the Laplacian.

Having dealt with scalability of λ, we now turn to scalability of the nodal approximation $\lambda_{a,X}$ of (1). To match the scalability order s of λ, we should assume the same h power for $\lambda_{a,X}$, and consider

$$h^{-s}\lambda_{a,X}(u(h\cdot)) = \sum_{j=1}^{M} a_j h^{-s} u(hx_j) = \lambda_{ah^{-s},hX}(u)$$

for all $u \in U$ and $0 < h \le 1$. This is the right notion of scalability for the approximation, but now we need the h dependence and refrain from setting this equal to $\lambda_{a,X}(u)$ like in Definition 1.

Definition 2. *1. An approximation (1) to a scalable functional λ of scaling order s is* scalable *of the same order, if the error functional is scalable of order s, i.e.*

$$\varepsilon_h(u) := \lambda(u) - \lambda_{ah^{-s},hX}(u) = h^{-s}(\lambda - \lambda_{a,X})(u(h\cdot)) = h^{-s}\varepsilon_1(u(h\cdot)) \quad (4)$$

for all $u \in U$, $0 < h \le 1$.

2. A scalable approximation (4) will be called a stencil.

3. If an approximation (1) is given for $h = 1$, and if the functional λ has scaling order s, the transition to (4) by using weights $a_j h^{-s}$ in the scaled case will be called enforced *scaling.*

A standard example is the five-point star approximation

$$-\Delta u(0,0) \approx \frac{1}{h^2}(4u(0,0) - u(0,h) - u(0,-h) - u(h,0) - u(-h,0))$$

to the Laplacian in 2D, and all other notions of generalized divided differences that apply to scaled node sets hX.

The scaled form in (4) allows the very simple error bound

$$|\varepsilon_h(u)| \le h^{-s}\|\lambda - \lambda_{a,X}\|_{U^*}\|u(h\cdot)\|_U \text{ for all } u \in U$$

that is useful if $\|u(h\cdot)\|_U$ is accessible and behaves nicely for $h \to 0$.

Weights of scalable approximations can be calculated at large scales and then scaled down by multiplication. This bypasses instabilities for small h and saves a lot of computational work, in particular if applications work on multiple scales or if meshless methods use the same geometric pattern of nodes repeatedly, e.g. in Meshless Local Petrov Galerkin [3] techniques.

However, *optimal* approximations in Sobolev spaces will not be scalable. This is why the rest of the paper studies how close scalable approximations come to the optimal ones analyzed in [12].

3 Optimal Convergence on Polynomials

We first relate the approximation error of nodal approximations to exactness on polynomials and assume that a scalable functional λ of scaling order s is given that is applicable to all d-variate polynomials. This will be true, for instance, in all Sobolev spaces $W_2^m(\Omega)$ for bounded scalable domains $\Omega \subset \mathbb{R}^d$. The space of all real-valued d-variate polynomials up to order q will be denoted by $\mathscr{P}_q^d$, and for a given node set $X \subset \mathbb{R}^d$ and a functional λ we define

$$q_{max}(\lambda, X) = \max\{q \,:\, \lambda - \lambda_{a,X} = 0 \text{ on } \mathscr{P}_q^d \text{ for some } a \in \mathbb{R}^{|X|}\}$$

to be the maximal possible *polynomial exactness order* (abbreviated by PEO in the figures of the examples) of a nodal approximation (1) to λ based on X.

Theorem 1. *Consider a fixed set $X \subset \mathbb{R}^d$ and a functional λ. If a sequence of general nodal approximations $\lambda_{a(h),hX}$ converges to λ on a space spanned by finitely many monomials, then X admits an approximation to λ that is exact on these monomials.*

Proof. Due to

$$\lambda(x^\alpha) - \lambda_{a(h),hX}(x^\alpha) = \lambda(x^\alpha) - \lambda_{a(h)h^{|\alpha|},X}(x^\alpha), \tag{5}$$

convergence of functionals $\lambda_{a(h),hX}$ to λ on a set of monomials implies that the error of the best approximation to λ by functionals $\lambda_{a,X}$, restricted to the space spanned by those monomials, is zero. □

We now know an upper bound for the maximal order of polynomials for which approximations can be convergent, if X and λ are fixed. This order can be achieved for scalable stencils:

Theorem 2. *If all polynomials are in U, the convergence rate of a scalable stencil of scaling order s based on a point set X on all polynomials is exactly $q_{max}(\lambda, X) - s$ if the stencil is exact on $\mathscr{P}_q^d$ for $q = q_{max}(\lambda, X)$. The convergence rate on all of U is bounded above by $q_{max}(\lambda, X) - s$.*

Proof. We apply (5) in the scalable situation and get

$$h^{-s}\lambda((hx)^\alpha) - h^{-s}\lambda_{a,X}((hx)^\alpha) = h^{-s+|\alpha|}\left(\lambda(x^\alpha) - \lambda_{a,X}(x^\alpha)\right),$$

proving the assertion. □

Consequently, if a node set $X = \{x_1, \ldots, x_M\}$ is given, if the application allows all polynomials, and if one wants a scalable stencil, the best one can do is to take a stencil with maximal order $q_{max}(\lambda, X)$ of polynomial exactness. It will lead to a scalable stencil with the optimal convergence rate among all approximations. Additional tricks cannot improve that rate, but it can be smaller due to restricted smoothness of functions in U. This will be the topic of Section 4.

If exactness of order q is required in applications, one takes a basis $p_1, \ldots, p_Q$ of the space $\mathscr{P}_q^d$ of d-variate polynomials of order q with $Q = \dim \mathscr{P}_q^d = \binom{q+d-1}{d}$ and has to find a solution of the linear system

$$\lambda(p_k) = \sum_{j=1}^{M} a_j p_k(x_j),\ 1 \le k \le Q. \tag{6}$$

This may exist even in case $M < Q$, the simplest example being the five-point star in 2D for $\lambda(u) = \Delta u(0)$ which is exact of order 4, while $M = 5 < Q = 10$. For general point sets, there is no way around setting up and solving the above linear system.

If the system has a solution, we get a stencil by enforced scaling and with error

$$h^{-s}\lambda(u(h\cdot)) - h^{-s}\sum_{j=1}^{M} a_j u(hx_j)$$

which then is polynomially exact of order q and has convergence rate $k = q - s$, but only on polynomials. If U contains functions of limited smoothness, this convergence rate will not be attained for all functions in U. We shall prove in Section 4 that the convergence rate in $W_2^m(\Omega)$ for $\Omega \subseteq \mathbb{R}^d$ is limited by $m - s - d/2$, no matter how large the order q of polynomial exactness on X is.

To make this construction partially independent of the functionals, we add

Definition 3. *A finite point set $X = \{x_1, \ldots, x_M\} \subset \mathbb{R}^d$ has* polynomial reproduction *of order q, if all polynomials in $\mathscr{P}_q^d$ can be recovered from their values on X.*

Theorem 3. *If the set X allows polynomial reproduction of order q, then all admissible linear functionals of scaling order $s \le q$ have a stencil that is exact at least of order q, by applying λ to a Lagrange basis of $\mathscr{P}_q^d$. This stencil has convergence rate at least $q - s$ on polynomials.*

Proof. Let the set X allow polynomial reproduction of order q. Then, for $Q = \dim \mathscr{P}_q^d$, there are polynomials $p_1, \ldots, p_Q$ and a subset $Y = \{y_1, \ldots, y_Q\} \subseteq X$ such that the representation

$$p(x) = \sum_{j=1}^{Q} p(y_j) p_j(x) \text{ for all } p \in \mathscr{P}_q^d$$

holds, and the matrix of values $p_k(y_j)$, $1 \le j.k \le Q$ is the identity. This implies $Q \le M$, and the stencil satisfying

$$\lambda(p) = \sum_{j=1}^{Q} p(y_j)\lambda(p_j) \text{ for all } p \in \mathscr{P}_q^d$$

with weights $a_j := \lambda(p_j)$ is exact on $\mathscr{P}_q^d$. The rest follows like above. □

But note that the five-point star is an example of an approximation on a set that has polynomial reproduction only of order 2, while it has a scalable stencil for the Laplacian that is exact on polynomials of order up to 4 and convergent of rate 2. The application of Theorem 3 would require polynomial reproduction of order 4 for the same convergence rate.

In general, one can use the M given nodes for getting exactness on polynomials of maximal order, and then there can be additional degrees of freedom because the $Q \times M$ linear system (6) may be nonuniquely solvable. The paper [13] deals with various techniques to use the additional degrees of freedom, e.g. for minimizing the ℓ_1 norm of the weights. In all cases the result is scalable and then this paper applies as well. On the other hand, the paper [12] focuses on non-scalable approximations induced by kernels. Both papers perform their convergence analysis mainly for single approximations. While this paper focuses on convergence rates in Sobolev spaces, [12] considers Hölder spaces and Sobolev spaces W_∞^r. A third way to use additional degrees of freedom is to take optimal stencils for polyharmonic kernels in Beppo-Levi spaces, see Section 5.

But before we go over from polynomials to these spaces, we remark that many application papers use meshless methods to solve problems that have true solutions u^* with rapidly convergent power series representations (see e.g [23] for a recent example with $u^*(x,y) = \exp(ax+by)$). In such cases, a high order of polynomial exactness pays off, but as soon as the problem is treated in Sobolev space, this advantage is gone. A truly worst-case analysis of nodal meshless methods is in [30].

This discussion showed that on polynomials one can get stencils of arbitrarily high convergence rates, provided that there are enough nodes to ensure exactness on high-degree polynomials. For working on spaces of functions with limited smoothness, the latter will limit the convergence rate of the stencil, and we want to show how.

4 Optimal Convergence in Sobolev Spaces

Our goal is to reach the optimal convergence rates in Sobolev spaces via cheap, scalable, and stable stencils, and for this we need to know those rates. But before

that, we want to eliminate the difference between local and global Sobolev spaces, as far as convergence *rates* are concerned.

Local Sobolev functionals are global ones due to $W_2^m(\Omega)^* \subset W_2^m(\mathbb{R}^d)^*$ that follows from $W_2^m(\Omega) \supset W_2^m(\mathbb{R}^d)$ for Lipschitz domains. This implies that we can evaluate the norm of each functional $\lambda \in W_2^m(\Omega)^*$ in $W_2^m(\mathbb{R}^d)^*$ via the kernel, up to a fixed multiplicative constant.

For the other way round and in the scalable case, we consider the subspace L_Ω of all point-based functionals $\lambda_{a,X} \in W_2^m(\mathbb{R}^d)^*$ with sets $X \subset \Omega$ and $a \in \mathbb{R}^{|X|}$ for a scalable domain $\Omega \subset \mathbb{R}^d$ and form its closure $\mathscr{L}_\Omega$ under the kernel-based $W_2^m(\mathbb{R}^d)^*$ norm. Exactly these functionals are those that we study here. Since the spaces $W_2^m(\mathbb{R}^d)$ and $W_2^m(\Omega)$ are norm-equivalent, the limit process is the same in $W_2^m(\Omega)$, and therefore we have that $\mathscr{L}_\Omega \subset W_2^m(\Omega)^*$.

Theorem 4. *The functionals considered here are always in the space $\mathscr{L}_\Omega \subset W_2^m(\Omega)^*$, and their norm can be evaluated in $W_2^m(\mathbb{R}^d)^*$ up to a space- and domain-dependent constant. The convergence rates in $W_2^m(\Omega)^*$ and $W_2^m(\mathbb{R}^d)^*$ are the same.* □

In Section 5 we shall extend this argument to Beppo-Levi spaces.

Theorem 5. *The convergence rate of any nodal approximation to a scalable functional λ of scalability order s on $W_2^m(\mathbb{R}^d)$ with $m > d/2$ is at most $m - s - d/2$.*

Proof. We need at least $m > d/2$ to let the nodal approximations $\lambda_{a,X}$ of (1) to be well-defined. Then we take a "bump" function $v \in W_2^m(\mathbb{R}^d)$ that vanishes on X and has $\lambda(v) \neq 0$.

Now we scale and consider $\lambda_{a(h),hX}$ as an approximation on hX with error functional

$$\varepsilon_h = \lambda - \lambda_{a(h),hX}.$$

Then

$$\begin{aligned} \varepsilon_h(v(\cdot/h)) &= \lambda(v(\cdot/h)) - \lambda_{a(h),hX}(v(\cdot/h)) \\ &= h^{-s}\lambda(v) - 0 \end{aligned}$$

and

$$\begin{aligned} \|v(\cdot/h)\|^2_{W_2^m(\mathbb{R}^d)} &= \sum_{|\alpha|\le m} \int_{\mathbb{R}^d} |D^\alpha(v(\cdot/h))|^2 \\ &= \sum_{|\alpha|\le m} h^{-2|\alpha|} \int_{\mathbb{R}^d} |D^\alpha(v)(x/h)|^2 dx \\ &= h^d \sum_{|\alpha|\le m} h^{-2|\alpha|} \int_{\mathbb{R}^d} |D^\alpha(v)(y)|^2 dy \\ &\le h^{d-2m} \|v\|^2_{W_2^m(\mathbb{R}^d)} \end{aligned}$$

leading to

$$\begin{aligned}
\|\varepsilon_h\|_{W_2^m(\mathbb{R}^d)^*} &= \sup_{u\in W_2^m(\mathbb{R}^d)\setminus\{0\}} \frac{|\varepsilon_h(u)|}{\|u\|_{W_2^m(\mathbb{R}^d)}} \\
&\geq \frac{|\varepsilon_h(v(\cdot/h))|}{\|v(\cdot/h)\|_{W_2^m(\mathbb{R}^d)}} \\
&\geq h^{-s}\frac{|\lambda(v)|}{\|v(\cdot/h)\|_{W_2^m(\mathbb{R}^d)}} \\
&\geq h^{m-s-d/2}\frac{|\lambda(v)|}{\|v\|_{W_2^m(\mathbb{R}^d)}}.
\end{aligned}$$

□

This holds for all weights, including the non-scalable optimal ones, and for all nodal point sets X.

Our next goal is to show that this rate is attainable for scalable stencils with sufficient polynomial exactness, in particular for optimal stencils calculated via polyharmonic kernels.

Theorem 6. *Let λ be a functional of scaling order s that is continuous on $W_2^\mu(\Omega)$ for some $\mu > d/2$, and let X allow a polynomially exact approximation to λ of of some order $q \geq \mu > d/2$. Then any scalable stencil for approximation of λ on X with that exactness has the optimal convergence rate $m-s-d/2$ in $W_2^m(\Omega)$ for all m with $\mu \leq m < q+d/2$. In case $m = q+d/2$, the rate is at least $m-s-d/2-\varepsilon = q-s-\varepsilon$ for arbitrarily small $\varepsilon > 0$.*

Proof. We first treat the case $m \leq q$. By the Bramble-Hilbert lemma [7], the error functional defined by

$$\varepsilon(u) = \lambda(u) - \lambda_{a,X}(u)$$

is continuous on $W_2^m(\Omega)$ and vanishes on $\mathscr{P}_m^d$. Then it has an error bound

$$|\varepsilon(u)| \leq \|\varepsilon\|_{W_2^m(\Omega)^*}|u|_{W_2^m(\Omega)} \text{ for all } u \in W_2^m(\Omega).$$

This leads to

$$\begin{aligned}
|h^{-s}\lambda(u(h\cdot)) - h^{-s}\lambda_{a,X}(u(h\cdot))| &= h^{-s}|\varepsilon(u(h\cdot))| \\
&\leq h^{-s}\|\varepsilon\|_{W_2^m(\Omega)^*}|u(h\cdot)|_{W_2^m(\Omega)} \\
&= h^{-s}\|\varepsilon\|_{W_2^m(\Omega)^*}h^{m-d/2}|u|_{W_2^m(h\Omega)} \\
&\leq h^{-s}\|\varepsilon\|_{W_2^m(\Omega)^*}h^{m-d/2}|u|_{W_2^m(\Omega)}
\end{aligned}$$

where we used

$$\begin{aligned} |u(h\cdot)|^2_{W_2^m(\Omega)} &= \sum_{|\alpha|=m} \int_\Omega |D^\alpha (u(h\cdot))(x)|^2 \, dx \\ &= h^{2m} \sum_{|\alpha|=m} \int_\Omega |D^\alpha (u)(hx)|^2 \, dx \\ &= h^{2m-d} \sum_{|\alpha|=m} \int_{h\Omega} |D^\alpha (u)(y)|^2 \, dy \\ &= h^{2m-d} |u|^2_{W_2^m(h\Omega)}. \end{aligned} \tag{7}$$

For the case $q \le m < q + d/2$ we repeat the argument, but now in $W_p^q(\Omega) \supseteq W_2^m(\Omega)$ for $p \in [2,\infty)$ with $q - d/p = m - d/2$. Because of $q \ge \mu$ we also have $W_p^q(\Omega) \subseteq W_2^\mu(\Omega)$, guaranteeing continuity on $W_p^q(\Omega)$. The corresponding proof steps are

$$\begin{aligned} |h^{-s}\lambda(u(h\cdot)) - h^{-s}\lambda_{a,X}(u(h\cdot))| &\le h^{-s} \|\varepsilon\|_{W_p^q(\Omega)^*} h^{q-d/p} |u|_{W_p^q(\Omega)}, \\ |u(h\cdot)|^p_{W_p^q(\Omega)} &= h^{pq-d} |u|^p_{W_p^q(\Omega)}. \end{aligned}$$

For $m = q + d/2$, the space $W_2^m(\Omega)$ is embedded in $W_p^q(\Omega)$ for arbitrary $p \in [2,\infty)$, and on that space we get the rate $q - s - d/p = m - s - d/2 - d/p$. □

Theorem 6 proves optimality of the convergence rate (2), and it shows that the optimal rate is attained by *scalable* stencils whose point sets allow polynomial exactness of some order larger than $m - d/2$.

In view of the *best compromise* situation, one can ask for the minimal polynomial exactness order q that allows the optimal convergence rate for fixed m and d. If $m - d/2$ is not an integer, this is $q := \lceil m - d/2 \rceil$ as in (3). In the exceptional case $m - d/2 \in \mathbb{N}$, the order $m - d/2 + 1$ is sufficient for the optimal rate, but order $m - d/2$ can come arbitrarily close to it. We shall deal with this situation in Sections 5 and 8.

Consequently, large orders of polynomial exactness will not pay off, if smoothness is the limiting factor. If the size of the point set X is the limiting factor, we get

Corollary 1. *Let λ be a functional of scaling order s which is continuous on $W_2^\mu(\Omega)$ with integer $\mu > d/2$, and let X allow a polynomially exact approximation to λ of of some order $q \ge \mu$. Then any scalable stencil for approximation of λ on X with that exactness has convergence rate at least $q - s$ in $W_2^m(\Omega)$ for all $m > q + d/2$.*

Proof. We repeat the proof of Theorem 6, but now on $W_2^q(\Omega)$ and get

$$\begin{aligned} |h^{-s}\lambda(u(h\cdot)) - h^{-s}\lambda_{a,X}(u(h\cdot))| &= h^{-s} |\varepsilon(u(h\cdot))| \\ &\le h^{-s} \|\varepsilon\|_{W_2^q(\Omega)^*} |u(h\cdot)|_{W_2^q(\Omega)}. \end{aligned}$$

Then we use (7) replacing m by q there, but insert functions $u \in W_2^m(\Omega)$ for $m > q + d/2$. Then the q-th derivatives in (7) will be continuous, proving

$$\begin{aligned} |u(h\cdot)|^2_{W_2^q(\Omega)} &= h^{2q} \sum_{|\alpha|=q} \int_\Omega |D^\alpha(u)(hx)|^2 \, dx \\ &\le Ch^{2q} \|u\|_{C^q(\Omega)}. \end{aligned}$$

Thus the convergence rate in $W_2^m(\Omega)$ is at least $q - s$. □

This argument used continuity of higher derivatives to bound local integrals, as in [12].

Note that Corollary 1 produces only integer or half-integer convergence rates while Theorem 6 allows general non-integer rates. We shall give examples in Section 8.

To summarize, we get convergence rates for scalable stencils as in Table 1. For the case in the second row, the optimal convergence behavior is not reached for order q, but for order $q+1$ by applying the first row. For given m and d, a scalable stencil with polynomial exactness order $\lfloor m - d/2 \rfloor + 1$ is sufficient for optimal convergence in $W_2^m(\Omega)$, $\Omega \subset \mathbb{R}^d$. By solving the system (6), such stencils are easy to calculate, but if the system is underdetermined, one should make good use of the additional degrees of freedom. This topic is treated in [13] by applying optimization techniques, while the next sections will focus on unique stencils obtained by polyharmonic kernels. Because the latter come close to the kernels reproducing Sobolev spaces, they should provide good approximations to the non-scalable optimal approximations in Sobolev spaces.

m and q	minimal rate	optimal rate
$m < q + d/2$	$m - s - d/2$	yes
$m = q + d/2$	$m - s - d/2 - \varepsilon$, $\varepsilon > 0$	no, $m - s - d/2 = q - s$
$m > q + d/2$	$q - s$	yes for $q = q_{max}(\lambda, X)$

Table 1: Convergence rates in $W_2^m(\mathbb{R}^d)$ for scalable stencils defined on $W_2^\mu(\mathbb{R}^d)$ with polynomial exactness $q \ge \mu > d/2$.

5 Polyharmonic Kernels

For $m - d/2 > 0$ real, we define the polyharmonic kernel

$$H_{m,d}(r) := (-1)^{\lfloor m-d/2 \rfloor + 1} \left\{ \begin{array}{ll} r^{2m-d} \log r, & 2m-d \text{ even integer} \\ r^{2m-d}, & \text{else} \end{array} \right\} \qquad (8)$$

up to a positive scalar multiple. This kernel is conditionally positive definite of order

$$q(m-d/2) := \lfloor m-d/2 \rfloor + 1.$$

For comparison, the Whittle-Matérn kernel generating Sobolev space $W_2^m(\mathbb{R}^d)$ is, up to a positive constant,

$$S_{m,d}(r) := K_{m-d/2}(r) r^{m-d/2}$$

with the modified Bessel function of second kind. The generalized d-variate Fourier transforms then are

$$\begin{aligned} \hat{H}_{m,d}(\omega) &= \|\omega\|_2^{-2m}, \\ \hat{S}_{m,d}(\omega) &= (1+\|\omega\|_2^2)^{-m}, \end{aligned}$$

up to positive constants, showing a similarity that we will not explore further at this point.

While $S_{m,d}$ reproduces $W_2^m(\mathbb{R}^d)$, the polyharmonic kernel $H_{m,d}$ reproduces the *Beppo-Levi* space $BL_{m,d}$. This has a long history, see e.g. [19, 27, 20, 39, 5, 21], but we take a shortcut here and refer the reader to the background literature. From the paper [20] of A. Iske we take the very useful fact that optimal approximations in Beppo-Levi spaces using polyharmonic kernels are always scalable and can be stably and efficiently calculated. We shall investigate the optimal convergence rate in Sobolev and Beppo-Levi space here, while [20] contains convergence rates in $C^m(\Omega)$.

A typical scale-invariance property of Beppo-Levi spaces is

$$\|u(h\cdot)\|_{BL_{m,d}} = h^{m-d/2}\|u\|_{BL_{m,d}} \text{ for all } u \in BL_{m,d}. \tag{9}$$

Note the similarity between the above formula and (7) used the proof of Theorem 6, because the classical $W_2^m(\mathbb{R}^d)$ seminorm coincides with the norm in $BL_{m,d}$.

Theorem 7. *Let a scalable approximation (1) of scaling order s be exact on the polynomials of some order $q \geq q(m-d/2) = \lfloor m-d/2 \rfloor + 1$ and assume that $\lambda - \lambda_{a,X}$ is in $BL_{m,d}^*$. Then this stencil has the exact convergence rate $m-s-d/2$ in $BL_{m,d}$.*

Proof. We evaluate the norm of the error functional after scaling via

$$\begin{aligned} \|\lambda - h^{-s}\lambda_{a,hX}\|_{BL_{m,d}^*} &= \sup_{\|u\|_{BL_{m,d}}\leq 1} |\lambda(u) - h^{-s}\lambda_{a,hX}(u)| \\ &= h^{-s} \sup_{\|u\|_{BL_{m,d}}\leq 1} |\lambda(u(h\cdot)) - \lambda_{a,X}(u(h\cdot))| \\ &= h^{-s+m-d/2} \sup_{\|u(h\cdot)\|_{BL_{m,d}}\leq 1} |\lambda(u(h\cdot)) - \lambda_{a,X}(u(h\cdot))| \\ &= h^{-s+m-d/2}\|\lambda - \lambda_{a,X}\|_{BL_{m,d}^*} \end{aligned}$$

using that (9) implies that the unit balls of all u and all $u(h\cdot)$ are the same up to a factor. □

Corollary 2. *Polynomial exactness of more than order $\lfloor m-d/2\rfloor+1$ does not pay off in a higher convergence rate in Beppo-Levi space $BL_{m,d}$.* □

Corollary 3. *Let a point set $X=\{x_1,\ldots,x_M\}\subset\Omega\subset\mathbb{R}^d$ be given such that there is some approximation (1) that is exact on polynomials of order $\lfloor m-d/2\rfloor+1$ and that has $\lambda-\lambda_{a,X}\in BL^*_{m,d}$. Then there is a weight vector $a^*\in\mathbb{R}^M$ that minimizes $\|\lambda-\lambda_{a,X}\|_{BL^*_{m,d}}$ under all competing approximations, and the resulting stencil is $BL_{m,d}$-optimal under all stencils of at least that polynomial exactness.* □

By applying Theorem 6, we get

Corollary 4. *One can use optimal scalable stencils obtained via polyharmonic kernels $H_{m,d}$ to get optimal convergence rates in $W_2^m(\Omega)$ for $\Omega\subset\mathbb{R}^d$, provided that the underlying sets allow exactness on polynomials of order $q(m-d/2)=\lfloor m-d/2\rfloor+1$.* □

If $m-d/2$ is not an integer, the above order is smallest possible for optimal convergence. For $m-d/2$ integer, we have

$$q(m-d/2)=\lfloor m-d/2\rfloor+1=m-d/2+1,$$

and Theorem 6 suggests that we could come arbitrarily close to the optimal convergence rate if we use order $q=m-d/2$. But then we cannot use the polyharmonic kernel $H_{m,d}$.

However, there is a workaround. We construct a scalable stencil via the polyharmonic kernel $H_{m',d}$ for $m-1\le m'<m$ using polynomial exactness of order $q(m'-d/2)=q$. By Theorem 6 this yields a convergence rate at least $m-s-d/2-\varepsilon$ for all $\varepsilon>0$, no matter how m' was chosen.

Corollary 5. *For the special situation $m=q+d/2$ in Table 1 there is a scalable stencil with polynomial exactness order q, based on a polyharmonic kernel, that has convergence rate at least $m-s-d/2-\varepsilon$ for all $\varepsilon>0$.* □

6 Stable Error Evaluation

In the most interesting cases, the leading term of the error of a scalable stencil in Sobolev space can be stably calculated via polyharmonic kernels. To prove this, we show now that the polyharmonic kernels $H_{m,d}$ arise naturally as part of the kernels $S_{m,d}$ reproducing Sobolev space $H^m(\mathbb{R}^d)$. The latter have expansions as series in r, beginning with a finite number of even powers with alternating signs. Such even powers, when written as $r^{2k}=\|x-y\|_2^{2k}$ are polynomials in x and y. After these even powers, the next term is a polyharmonic kernel:

Theorem 8. *The first non-even term in the expansion of* $\sqrt{\frac{2}{\pi}}K_{n+1/2}(r)r^{n+1/2}$ *into powers of* r *for integer* $n \geq 0$ *is the polyharmonic kernel*

$$r^{2n+1}\frac{(-1)^{n+1}}{(2n+1)(2n-1)(2n-3)\cdots 1} = r^{2n+1}\frac{(-1)^{n+1}2^n n!}{(2n+1)!}.$$

The first non-even term in the expansion of $K_n(r)r^n$ *for integer* $n \geq 0$ *is the polyharmonic kernel* $(-1)^{n+1}r^{2n}\log(r)\frac{2^{-n}}{n!}$.

Proof. Equation 10.39.2 of [25] has $n = 0$ of

$$\sqrt{\frac{2}{\pi}}K_{n+1/2}(r)r^{n+1/2} = q_n(r) = e^{-r}p_n(r)$$

with a polynomial p_n of degree at most n, $p_0(r) = 1$, $q_0(r) = e^{-r}$. It can easily be shown that $rp_{n-1}(r) + p_n'(r) = p_n(r)$ holds, using the derivative of the above expression, and similarly one gets

$$-rq_{n-1}(r) = q_n'(r)$$

from that derivative formula. If we make it explicit by

$$q_n(r) =: \sum_{j=0}^{\infty} q_{j,n}r^j,$$

we get

$$\begin{aligned} -q_{k-1,n-1} &= q_{k+1,n}(k+1), k, n \geq 1 \\ 0 &= q_{1,n},\ n \geq 1. \end{aligned}$$

The assertion $q_{2k-1,n} = 0$ for $1 \leq k \leq n$ is true for $k = 1$ and all $n \geq 1$. Assume it to be true for k and all $n \geq k$. Then for all $n \geq k \geq 1$,

$$0 = -q_{2k-1,n} = q_{2k+1,n+1}(2k+1), 2k \geq 1, n \geq 0$$

proves the assertion. The first odd term of the kernel expansion is $q_{2n+1,n}r^{2n+1}$, and its coefficient has the recursion

$$-q_{2n-1,n-1} = q_{2n+1,n}(2n+1), n \geq 1.$$

For the other case we use equation (10.31.1) of [25] in shortened form as

$$K_n(z)z^n = p_n(z^2) + (-1)^{n+1}z^n\log(z/2)I_n(z)$$

with an even power series $p_n(z^2)$, and due to (10.25.2) of [25] we have $I_n(z) = z^n q_n(z^2)$ with an even power series $q_n(z^2)$ with $q_n(0) = \frac{2^{-n}}{n!}$. Thus

$$K_n(z)z^n = p_n(z^2) + (-1)^{n+1}z^{2n}\log(z/2)q_n(z^2),$$

and the first non-even term of the expansion of $K_n(r)r^n$ is the polyharmonic kernel

$$(-1)^{n+1}r^{2n}\log(r)q_n(0) = (-1)^{n+1}r^{2n}\log(r)\frac{2^{-n}}{n!}.$$

□

We now are ready to show that a good approximation of the error in Sobolev space can be calculated stably via the error in Beppo-Levi space, i.e. via polyharmonic kernels:

Theorem 9. *Assume a scalable stencil of scalability order s on a set $X \subset \mathbb{R}^d$ to be given with polynomial exactness q. For all integer m with $\lfloor m-d/2 \rfloor + 1 \leq q$, its error norm can be evaluated on all Beppo-Levi spaces $BL_{m,d}$ and on Sobolev space $W_2^m(\mathbb{R}^d)$. The convergence rate in both cases then is $m-s-d/2$, and the quotient of errors converges to 1 for $h \to 0$, if the scalar factors in the Sobolev and polyharmonic kernel are aligned properly, namely as given in Theorem 8.*

Proof. The squared norm of the stencil's error functional can be evaluated on Sobolev space $W_2^m(\mathbb{R}^d)$ by

$$\begin{aligned} & \varepsilon(h)^x\varepsilon(h)^y K(x,y) \\ = \; & h^{-2s}\left(\lambda^x\lambda^y K(hx,hy) - 2\sum_{j=1}^{M} a_j\lambda^y K(hx_j,hy)\right. \\ & \left. + -2\sum_{j,k=1}^{M} a_j a_k \lambda^y K(hx_j,hx_k)\right) \end{aligned}$$

where we used $K(x,y)$ as a shortcut for $K_{m-d/2}(\|x-y\|_2)\|x-y\|_2^{m-d/2}$ and ignore scalar multiples. Now we insert the series expansions of Theorem 8. For odd d and $m-d/2 = n+1/2$ we have, up to constant factors,

$$K_{m-d/2}(r)r^{m-d/2} = \sum_{j=0}^{m-d/2-1/2} f_{2j}r^{2j} + f_{2m-d}r^{2m-d} + \sum_{k>2m-d} f_k r^k$$

and

$$K_{m-d/2}(hr)(hr)^{m-d/2} = \sum_{j=0}^{m-d/2-1/2} f_{2j}h^{2j}r^{2j} + f_{2m-d}h^{2m-d}r^{2m-d} + \sum_{k>2m-d} f_k h^k r^k.$$

If we hit this twice with $\varepsilon(h)$, i.e. forming

$$\|\varepsilon(h)\|^2_{H^m(\mathbb{R}^d)} = \varepsilon(h)^x\varepsilon(h)^y K(h\|x-y\|_2),$$

all even terms with exponents $2j < 2q = 2p + 2s > 2m - d$ go away [29], and we are left with the polyharmonic part and higher-order terms. The odd ones are all polyharmonic, and the even ones remain only from exponent $2q = 2p + 2s > 2m - d$ on, i.e. they behave like h^{2m-d+1} or higher-order terms. The polyharmonic terms $f_{2m-d+2k} h^{2m-d+2k} r^{2m-d+2k}$ representing $BL_{m+k,d}$ require polynomial exactness of order $m - d/2 + 1/2 + k$ which is satisfied for $0 \leq k < q - m + d/2$, and double action of the error functional on these terms has a scaling law of $h^{2m+2k-2s-d}$. This means that the dominating term is the one with $k = 0$, and the squared error norm behaves like $h^{2m-d-2s}$ as in the $BL_{m,d}$ case.

Now we treat even dimensions, and use the expansion

$$K_{m-d/2}(r) r^{m-d/2} = \sum_{j=0}^{\infty} f_{2j} r^{2j} + g_{2m-d} \log(r) r^{2m-d} + \log(r) \sum_{2k>2m-d} g_{2k} r^{2k}$$

up to constant factors. With scaling, it reads as

$$\begin{aligned}
& K_{m-d/2}(hr) h^{m-d/2} r^{m-d/2} \\
= & \sum_{j=0}^{\infty} f_{2j} h^{2j} r^{2j} + g_{2m-d} \log(hr) h^{2m-d} r^{2m-d} + \log(hr) \sum_{2k>2m-d} g_{2k} h^{2k} r^{2k} \\
= & \sum_{j=0}^{\infty} f_{2j} h^{2j} r^{2j} + g_{2m-d} h^{2m-d} \log(r) r^{2m-d} + g_{2m-d} \log(h) h^{2m-d} r^{2m-d} \\
& + \sum_{2k>2m-d} g_{2k} h^{2k} r^{2k} \log(r) + \sum_{2k>2m-d} g_{2k} h^{2k} \log(h) r^{2k}
\end{aligned}$$

We now have $q = p + s \geq 2m - d + 2$ and hitting the scaled kernel twice will annihilate all even powers up to and including exponents $2j < 2q = 2p + 2s \geq 2m - d + 2$, i.e. the remaining even powers scale like $h^{2m-d+2} \log(h)$ or higher. The rest is a sum of polyharmonic kernels $H_{m+k,d}$ for $k \geq 0$, and we know the scaling laws of them, if the stencil has enough polynomial exactness. Again, the term with $k = 0$ is the worst case, leading to a summand of type $h^{2m-d-2s}$ in the squared norm of the error that cannot be cancelled by the other terms of higher order. □

7 Stencil Convergence

Here, we prove that the renormalized weights of the optimal non-scalable approximations in Sobolev space converge to the weights of a scalable stencil.

Theorem 10. *Consider the $W_2^m(\mathbb{R}^d)$-optimal approximation weights $a^*(h)$ on a set $X \subset \mathbb{R}^d$ for a functional of scaling order s. Assume that X allows a unique scalable stencil with weights $\hat{a}$ that is exact on polynomials of order q. Then*

$$\|a^*(h) h^s - \hat{a}\|_\infty \leq C h^{m-q+1-d/2}$$

if $m-d/2<q$, *and*

$$\|a^*(h)h^s-\hat{a}\|_\infty \le Ch^1$$

if $m-d/2\ge q$.

Proof. We consider the uniquely solvable system of polynomial exactness as

$$\sum_{j=1}^{M}\hat{a}_j x_j^\alpha=\lambda(x^\alpha),\ 0\le|\alpha|<q$$

and in scaled form as

$$\sum_{j=1}^{M}h^{-s}\hat{a}_j(hx_j)^\alpha=\lambda(x^\alpha),\ 0\le|\alpha|<q$$

which is the unscaled system where the equation for x^α is multiplied by $h^{|\alpha|-s}$, namely

$$\sum_{j=1}^{M}h^{-s}\hat{a}_j(hx_j)^\alpha=h^{|\alpha|-s}\lambda(x^\alpha)=\lambda(x^\alpha),\ 0\le|\alpha|<q$$

which is no contradiction because scaling order s implies $\lambda(x^\alpha)=0$ for $|\alpha|\ne s$. Then we insert the rescaled optimal Sobolev weights into the unscaled system to get

$$\begin{aligned}
& h^s\textstyle\sum_{j=1}^{M}a_j^*(h)x_j^\alpha\\
= \;& h^{s-|\alpha|}\textstyle\sum_{j=1}^{M}a_j^*(h)(hx_j)^\alpha\\
= \;& h^{s-|\alpha|}\lambda_{a^*(h),hX}(x^\alpha)\\
= \;& h^{s-|\alpha|}(\lambda_{a^*(h),hX}(x^\alpha)-\lambda(x^\alpha))+h^{s-|\alpha|}\lambda(x^\alpha)\\
= \;& h^{s-|\alpha|}(\lambda_{a^*(h),hX}(x^\alpha)-\lambda(x^\alpha))+\lambda(x^\alpha)
\end{aligned}\tag{10}$$

and

$$\textstyle\sum_{j=1}^{M}(h^sa_j^*(h)-\hat{a}_j)x_j^\alpha \;=\; h^{s-|\alpha|}(\lambda_{a^*(h),hX}(x^\alpha)-\lambda(x^\alpha)).$$

If we insert the convergence rate $m-s-d/2$ for the optimal Sobolev approximation in the case $m-s-d/2<q-s$ or $m-d/2<q$, the right-hand side of this system converges to zero with rate $m-|\alpha|-d/2\ge m-(q-1)-d/2\ge 1$ and this implies

$$h^sa_j^*(h)-\hat{a}_j=\mathcal{O}(h^{m-(q-1)-d/2})\text{ for }h\to 0.\tag{11}$$

If we have $m-d/2\ge q$, we insert the rate $q-s$ and get the rate $q-|\alpha|\ge 1$ for the right-hand side. □

8 Examples

First, we demonstrate numerically that the convergence rate

$$\min(m-d/2-s, q_{max}(\lambda, X)-s)$$

for approximations in $W_2^m(\mathbb{R}^d)$ to functionals $\lambda \in W_2^m(\mathbb{R}^d)^*$ with scaling order s is optimal, even among unscaled approximations. This was verified in many cases including dimensions 2 and 3 using MAPLE© with extended precision. The number of decimal digits had to be beyond 100 in extreme situations. All the loglog plots of $\|\varepsilon(h)\|_{W_2^m(\mathbb{R}^d)}$ versus h show the standard linear behaviour for $h \to 0$, if enough decimal digits are used and if started with small h values. Therefore, they are suppressed here. Instead, we present convergence rate estimates by plotting

$$\frac{\log(\|\varepsilon_{h_{i+1}}\|_{W_2^m(\mathbb{R}^d)}) - \log(\|\varepsilon_{h_i}\|_{W_2^m(\mathbb{R}^d)})}{\log(h_{i+1}) - \log(h_i)}$$

against h_i.

For a specific case, we take $M = 18$ random points in 2D and approximate the Laplacian. Then $s = 2$ and $q_{max}(\lambda, X) = 5$ leading to the expected convergence rate $\min(m-3, 3)$ as a function of smoothness. Figure 1 shows the cases $m = 3.75$ and $m = 6.25$ with the expected rates 0.75 and 2, respectively. These correspond to situations where either smoothness m or size of X restrict the convergence rate.

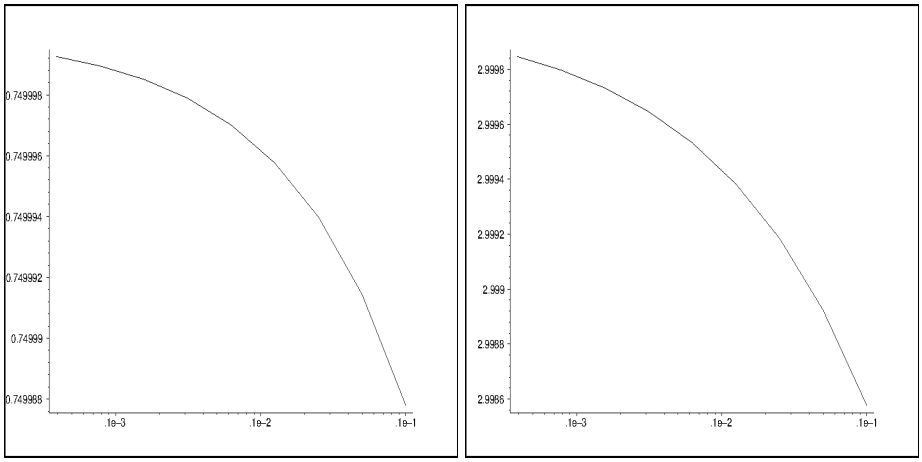

Figure 1: Convergence rate estimates of the optimal ε_h in $W_2^{3.75}(\mathbb{R}^2)$ and $W_2^{6.25}(\mathbb{R}^2)$ approximating the Laplacian on 18 general points as function of h

For illustration of the optimal compromise situation in (3), Figure 2 shows the convergence rate 1 for approximation of the Laplacian in 3D on only 10 points

in general position assuming smoothness $m = 4.5$. By Table 1 we expect a convergence rate between $m - s - d/2 - \varepsilon = 1 - \varepsilon$ and 1 for all $\varepsilon > 0$ when using polynomial exactness order $q = m - d/2 = 3$, but the true optimal convergence could be like $h\log(h)$. The issue cannot be visually decided.

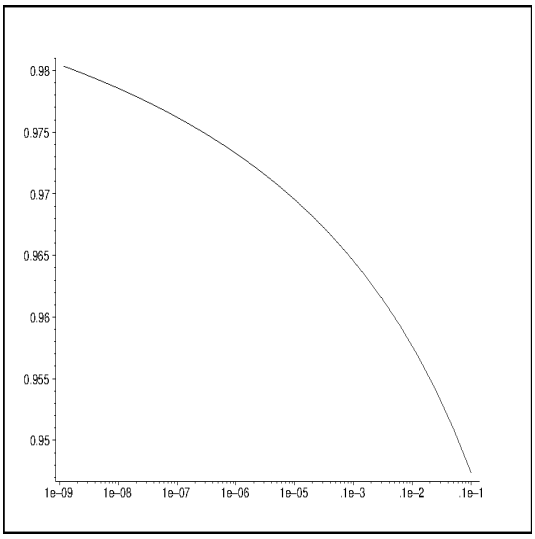

Figure 2: Convergence rate estimates of the optimal ε_h in $W_2^{4.5}(\mathbb{R}^3)$ approximating the Laplacian on 10 general points as function of h

Test runs with the scalable approximations based on polynomial exactness show exactly the same behaviour, since they have the same convergence rate. To illustrate the ratio between the errors of scalable polyharmonic stencils and unscaled optimal approximations, Figure 3 shows the error ratio in the 2D equilibrium case with 10 points and $m = q = 4$, tending to 1 for $h \to 0$. The same remark as for the $m = 4.5$, $d = 3$ case applies here.

To deal with the special situation of $m - d/2$ being an integer in Corollary 5 via polyharmonic kernels, we take 6 points in $\mathbb{R}^2$ with $q = q_{max} = 3$ for the Laplacian with optimal convergence rate $m - 2 - d/2 = 1$ for $m = 4$. Working in $BL_{4,2}$ would need 10 points. A unique scalable stencil is obtained from $BL_{m',2}$ with polynomial exactness order $q(m',2) = 3$ for all $3 \le m' < 4$ and the convergence rate is at least $m - s - d/2 - \varepsilon = 1 - \varepsilon$ for all $\varepsilon > 0$ by Table 1. The corresponding convergence rate estimate for $m' = 3.5$ is in Figure 4, and there is no visible $\log(h)$ factor.

To see whether a $\log(h)$ term can be present in the situation of integer $q = m - d/2$, we take $m = d = 2$, $q = 1$, $s = 0$, i.e. interpolation. We need just a single point $x \in \mathbb{R}^2$ with $\|x\|_2 = 1$ for exactness on constants. The kernel is $\phi(r) = rK_1(r) = 1 + \frac{1}{2}r^2\log r + \mathcal{O}(r^2)$ with $\phi(0) = 1$. The optimal recovery for

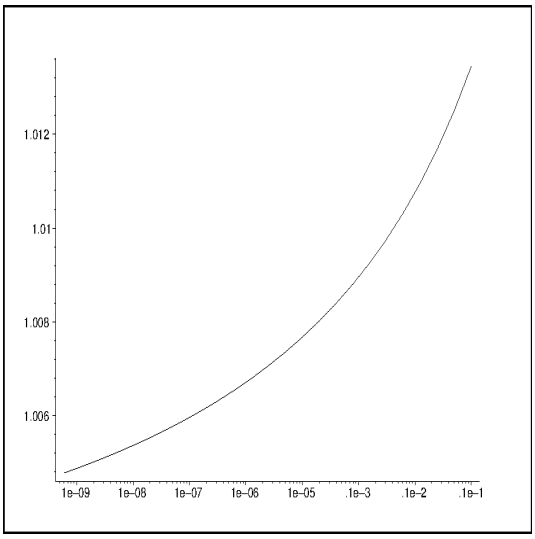

Figure 3: Quotient between errors of polyharmonic and optimal Sobolev approximations as functions of h

$\lambda(u) = u(0)$ from $u(hx)$ is the kernel interpolant, i.e. $u(hx)\phi(\|\cdot - hx\|_2)$, and the approximation error is

$$u(0) - u(hx)\phi(\|hx\|_2) = u(0) - u(hx)\phi(h).$$

In the dual of $W_2^2(\mathbb{R}^2)$ the square of the norm of the error functional is

$$\begin{aligned} \|\delta_0 - \phi(h)\delta_{hx}\|^2_{W_2^{2*}(\mathbb{R}^2)} &= \phi(0) - \phi(h)^2 \\ &= -h^2\log(h) + \mathscr{O}(h^2) \end{aligned}$$

due to MAPLE. Since the standard error bound

$$|u(0) - u(hx)\phi(h)| \le \|\delta_0 - \phi(h)\delta_{hx}\|_{W_2^{2*}(\mathbb{R}^2)}\|u\|_{W_2^2(\mathbb{R}^2)}$$

is sharp, and since we constructed the optimal recovery, we have that the convergence for $q = 1$ is only $h|\log(h)|^{1/2}$ and not like the optimal behaviour $h^{m-0-d/2} = h$ in Sobolev space $W_2^2(\mathbb{R}^2)$. To reach the optimal rate, we need a polynomial exactness order $q \ge 2$ by Table 1, i.e. at least three non-collinear points. For curiosity, note that the above analysis works for all even dimensions, provided that smoothness $m = 1 + d/2$ is varying accordingly.

The suboptimal nearest-neighbor interpolation by constants has

$$\begin{aligned} \|\delta_0 - \delta_{hx}\|^2_{W_2^{2*}(\mathbb{R}^2)} &= 2 - 2\phi(h) \\ &= -h^2\log(h) + \mathscr{O}(h^2) \end{aligned}$$

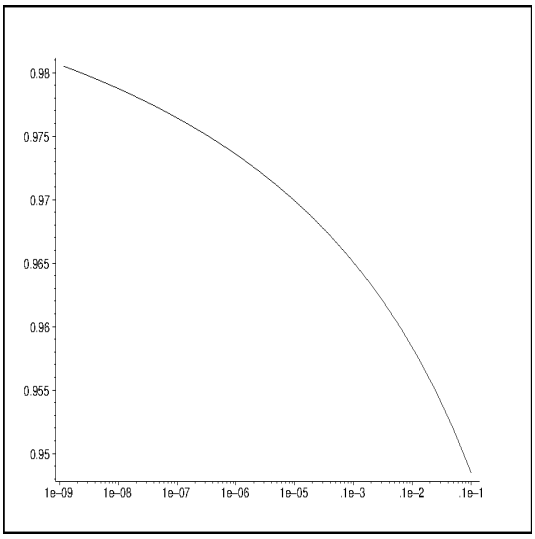

Figure 4: Convergence rate estimate for the error norm of ε_h in $W_2^4(\mathbb{R}^2)$ approximating the Laplacian on 6 general points by a stencil of polynomial exactness of order 3

and a more exact expansion via MAPLE shows that this is larger than the squared error for optimal one-point interpolation in $W_2^{1+d/2}(\mathbb{R}^d)$ by $\mathscr{O}(\log^2(h)h^4)$.

In several numerical examples we verified the stencil convergence proven in Theorem 10, but the observed convergence rates turned out to be better than the proven ones. In particular, choosing 15 points in general position in $\mathbb{R}^2$ with $q=5$ led to a convergence rate $\min(2,2m-10)$ for $m \geq 5$ instead of $\min(1,m-5)$ in Theorem 10. This seems to be a consequence of *superconvergence* [28, 31], but needs further work.

We now check approximation of the Laplacian in the native space of the Gaussian in Figure 5. This should behave like $m=\infty$ in (2) and thus show a convergence rate $q_{max}(\lambda,X)-s$. We used 256 decimal digits for that example and took a set of 30 random points in 2D. Then $q_{max}(\Delta,X)=7$ and the observed convergence rate is indeed $q_{max}-s=5$. Furthermore, this rate is attained already for a scalable stencil that is polynomially exact of order 7 on these points. We chose the optimal scalable polyharmonic stencil in $BL_{7,2}$ for this, and the ratio of the error norms was about 5. See [24] for a sophisticated way to circumvent the instability of calculating optimal non-scalable stencils for Gaussian kernels, but this paper suggests to use scalable stencils calculated via polyharmonic kernels instead.

We finally compare with approximations that optimize weights under the constraint of a fixed polynomial exactness [13].

The three point sets $X1$, $X2$, and $X3$ of [13] have 32 points in $[-1,+1]^2$ each,

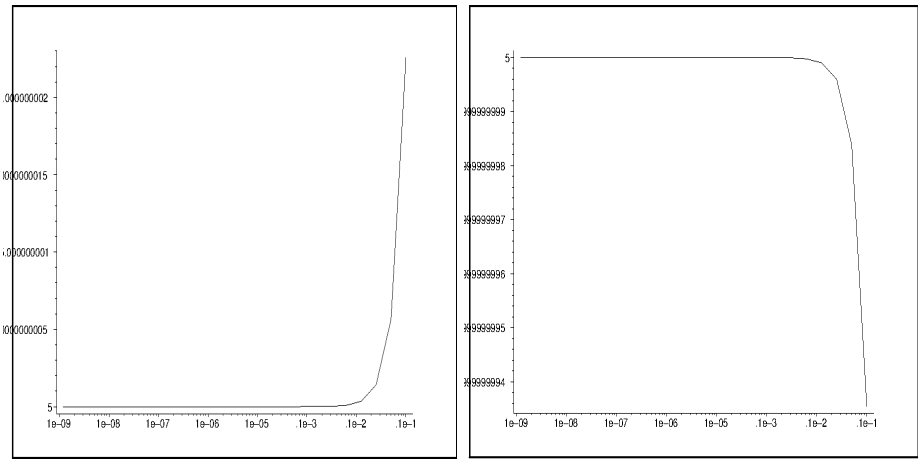

Figure 5: Gaussian native space convergence rate estimates for the error norms of the optimal and a polynomially exact stencil of order 7, approximating the Laplacian on 30 general points, as function of h

and the maximal possible order of polynomial reproduction in 2D is 7, if the geometry of the point set allows it. If everything works fine, this would result in convergence of optimal order 5 for the approximation of the Laplacian in Sobolev spaces of order $m \geq 8$, while the optimal rate for smaller m is $m-3$.

A simple Singular Value Decomposition of the 28x32 value matrix of polynomials of order 7 on these points reveals that the small singular values in the three cases are like in Table 2. This means that only $X1$ allows working for exactness order 7 without problems, while $X2$ suggests order 6 and $X3$ should still work with order 5. If users require higher polynomial exactness orders (PEO), there is a risk of numerical instabilities.

To demonstrate this effect, Figure 6 shows what happens if both the polyharmonic and the minimal-weight approximations are kept at order 7 for the set $X2$. As Figure 8 will show, the optimal Sobolev approximation stays at rate 4 for larger h and needs rather small h to show its optimal rate 5. In Figure 6, both the polyharmonic and the minimal-weight approximations perform considerably worse than the optimum. If we go to polynomial exactness order 6, we get Figure 7, and now both approximations are close to what the Sobolev approximation does, though the latter is not at its optimal rate yet. In Figure 8, the polyharmonic approximation is forced to stay at exactness order 7, while the weight-minimal approximation is taken at order 6 to allow more leeway for weight optimization. Now, in the same range as before, the weight-optimal approximation clearly outperforms the polyharmonic approximation. The same situation occurs on the set $X3$ under these circumstances, see Figure 9. Thus, for problematic point sets, the

polyharmonic approximation should get as much leeway as the minimal-weight approximation.

The most sensible choice on $X3$ is to fix the exactness orders to 5, and the results are in Figure 10. Both approximations cannot compete with the convergence rate 4 that the Sobolev approximation shows in this range of h. The latter is calculated using 128 digits and can still use the point set as one that allows polynomial reproduction of order 6. The other two approximations are calculated at 32 decimal digits and see the set $X3$ as one that allows reproduction of order 5 only. To get back to a stable situation, we should lower the Sobolev smoothness to $m = 6$ to get Figure 11. We then are back to a convergence rate like h^3 in all cases.

Set	> 0.002	$\in [2.0e-8, 3.6e-7]$	$< 5.0e-14$
X1	28	0	0
X2	25	3	0
X3	18	9	1

Table 2: Singular values for three point sets, for polynomial reproduction of order 7

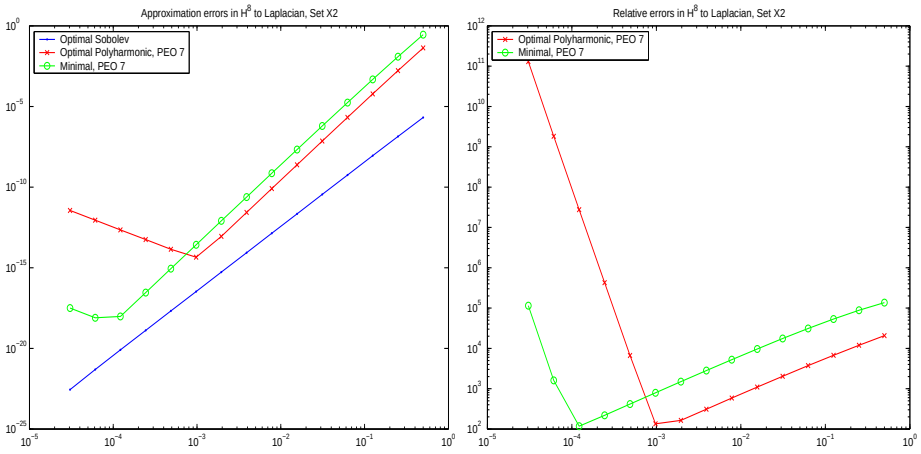
Approximation errors in H^8 to Laplacian, Set X2
Optimal Sobolev
Optimal Polyharmonic, PEO 7
Minimal, PEO 7
Relative errors in H^8 to Laplacian, Set X2
Optimal Polyharmonic, PEO 7
Minimal, PEO 7

Figure 6: Absolute and Sobolev-relative error norms in $W_2^8(\mathbb{R}^2)$ for approximations with polynomial exactness order (PEO) 7 on set $X2$

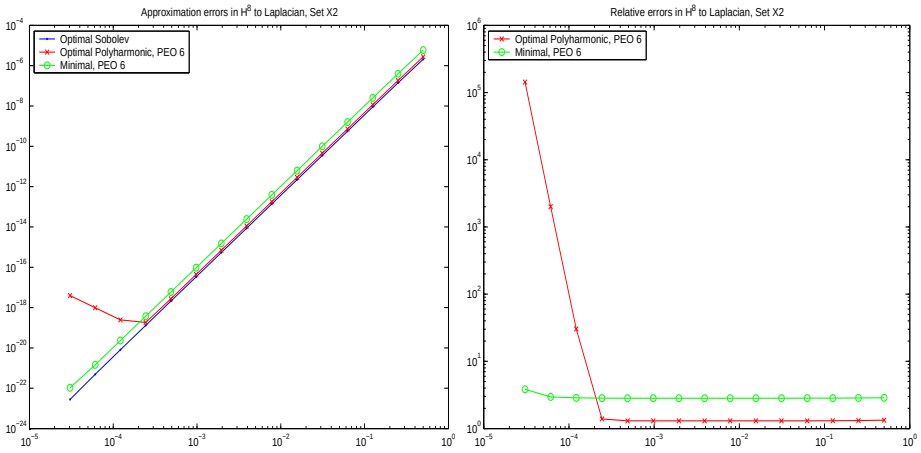
Approximation errors in H^8 to Laplacian, Set X2
Optimal Sobolev
Optimal Polyharmonic, PEO 6
Minimal, PEO 6
Relative errors in H^8 to Laplacian, Set X2
Optimal Polyharmonic, PEO 6
Minimal, PEO 6

Figure 7: Absolute and Sobolev-relative error norms in $W_2^8(\mathbb{R}^2)$ for approximations with polynomial exactness order 6 on set $X2$

9 Summary and Outlook

We established the optimal convergence rate (2) of nodal approximations in Sobolev spaces and proved that it can be attained for *scalable* approximations with sufficient polynomial exactness. But we did not investigate the factors in front of the rates. For highly irregular nodes, it might be reasonable to go for a smaller convergence rate, if the factor is much smaller than the one for the highest possible rate for that node configuration. This requires an analysis of how to use the additional degrees of freedom, and various possibilities for this are in [13]. On point sets that are badly distributed, it pays off to avoid the highest possible order of polynomial exactness, and to use the additional degrees of freedom for minimization of weights along the lines of [13] or to use optimal approximations by polyharmonic kernels at a smaller order of polynomial exactness.

The kernels reproducing Sobolev spaces $W_2^m(\mathbb{R}^d)$ have expansions into power series in $r = \|x-y\|_2$ that start with even powers of r until the polyharmonic kernel $H_{m,d}$ occurs. This shows that error evaluation in Sobolev spaces can be replaced asymptotically by evaluation in Beppo-Levi spaces, and it suggests that the errors of optimal kernel-based approximations should be close to the errors of optimal scalable stencils based on polyharmonic kernels. This occurred in various experiments (see Figure 3), but a more thorough investigation is needed.

Finally, the exceptional case $m - d/2 \in \mathbb{N}$ of the second row of Table 1 needs more attention. Approximating a functional with scaling order s by scalable stencils with the minimal polynomial exactness order $q = m - d/2$ leads to an unknown convergence behavior between rates $m - s - d/2 - \varepsilon$ and the optimal rate

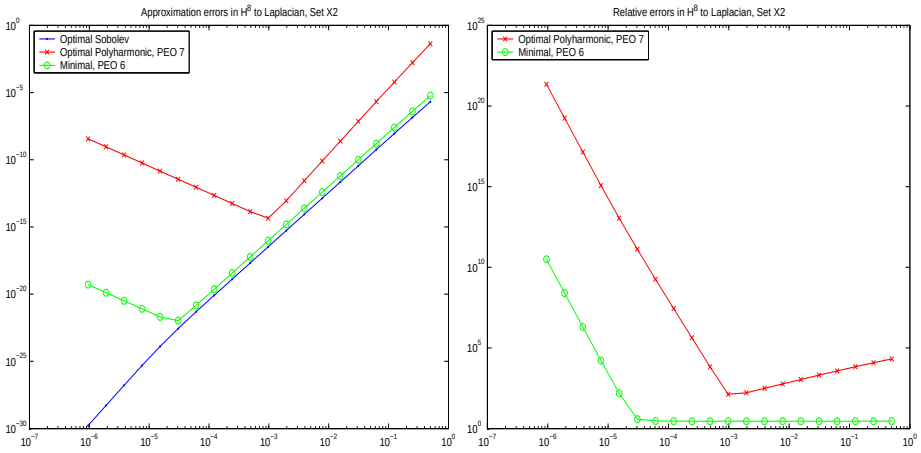
Approximation errors in H^8 to Laplacian, Set X2
Optimal Sobolev
Optimal Polyharmonic, PEO 7
Minimal, PEO 6
Relative errors in H^8 to Laplacian, Set X2
Optimal Polyharmonic, PEO 7
Minimal, PEO 6

Figure 8: Absolute and Sobolev-relative error norms in $W_2^8(\mathbb{R}^2)$ for polyharmonic approximation of order 7 and minimal approximation of order 6 on set $X2$

$m-s-d/2$ that is guaranteed for order $q+1 = m-d/2+1$. The convergence could be like $\mathcal{O}(h^{m-s-d/2}|\log(h)|^p)$, for instance, and we presented an example with $p = 1/2$ for $m = d = 2,\ s = 0$.

References

[1] T. Aboiyar, E.H. Georgoulis, and A. Iske. Adaptive ADER methods using kernel-based polyharmonic spline WENO reconstruction. *SIAM Journal on Scientific Computing*, 32:3251–3277, 2010.

[2] D. Agarwal and P. Basu. Development of a meshless local RBF-DQ solver and its applications in computational fluid dynamics. *Int. J. Numer. Methods Appl.*, 7(1):41–55, 2012.

[3] S. N. Atluri. *The meshless method (MLPG) for domain and BIE discretizations*. Tech Science Press, Encino, CA, 2005.

[4] V. Bayona, M. Moscoso, and M. Kindelan. Gaussian RBF-FD weights and its corresponding local truncation errors. *Eng. Anal. Bound. Elem.*, 36(9):1361–1369, 2012.

[5] R.K. Beatson, H.Q. Bui, and J. Levesley. Embeddings of Beppo-Levi spaces in Hölder-Zygmund spaces and a new method for radial basis function interpolation error estimates. *Journal of Approximation Theory*, 137:166–178, 2005.

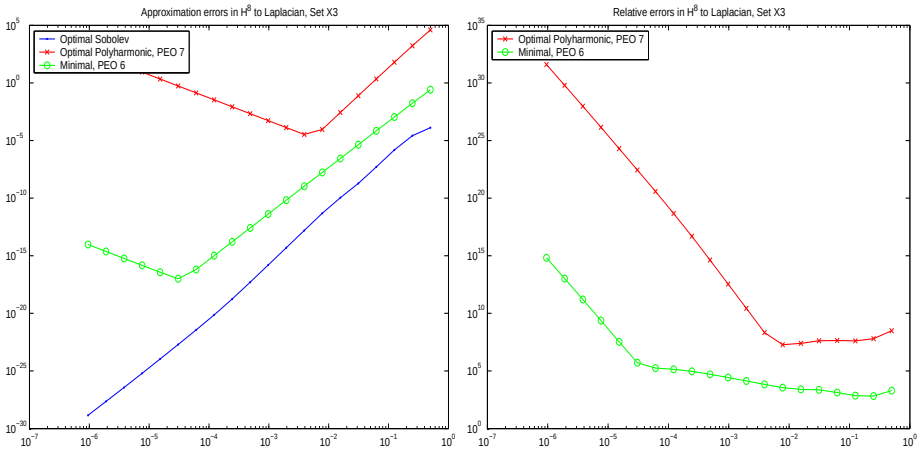
Approximation errors in H^8 to Laplacian, Set X3
Optimal Sobolev
Optimal Polyharmonic, PEO 7
Minimal, PEO 6
Relative errors in H^8 to Laplacian, Set X3
Optimal Polyharmonic, PEO 7
Minimal, PEO 6

Figure 9: Absolute and Sobolev-relative error norms in $W_2^8(\mathbb{R}^2)$ for polyharmonic approximation of order 7 and minimal approximation of order 6 on set $X3$

[6] T. Belytschko, Y. Krongauz, D.J. Organ, M. Fleming, and P. Krysl. Meshless methods: an overview and recent developments. *Computer Methods in Applied Mechanics and Engineering, special issue*, 139:3–47, 1996.

[7] J.H. Bramble and S.R. Hilbert. Estimation of linear functionals on Sobolev spaces with application to Fourier transforms and spline interpolation. *SIAM J. Numer. Anal.*, 7:112–124, 1970.

[8] G. Chandhini and Y. V. S. S. Sanyasiraju. Local RBF-FD solutions for steady convection-diffusion problems. *Internat. J. Numer. Methods Engrg.*, 72(3):352–378, 2007.

[9] O. Davydov and D.T. Oanh. Adaptive meshless centres and RBF stencils for Poisson equation. *J. Comput. Phys.*, 230:287–304, 2011.

[10] O. Davydov and D.T. Oanh. On the optimal shape parameter for Gaussian radial basis function finite difference approximation of the Poisson equation. *Comput. Math. Appl.*, 62:2143–2161, 2011.

[11] O. Davydov, D.T. Oanh, and H.X. Phu. Adaptive RBF-FD method for elliptic problems with point singularities in 2D. preprint, Univ. Gießen, 2016.

[12] O. Davydov and R. Schaback. Error bounds for kernel-based numerical differentiation. *Numerische Mathematik*, 132:243–269, 2016.

[13] O. Davydov and R. Schaback. Minimal numerical differentiation formulas. preprint, 2016.

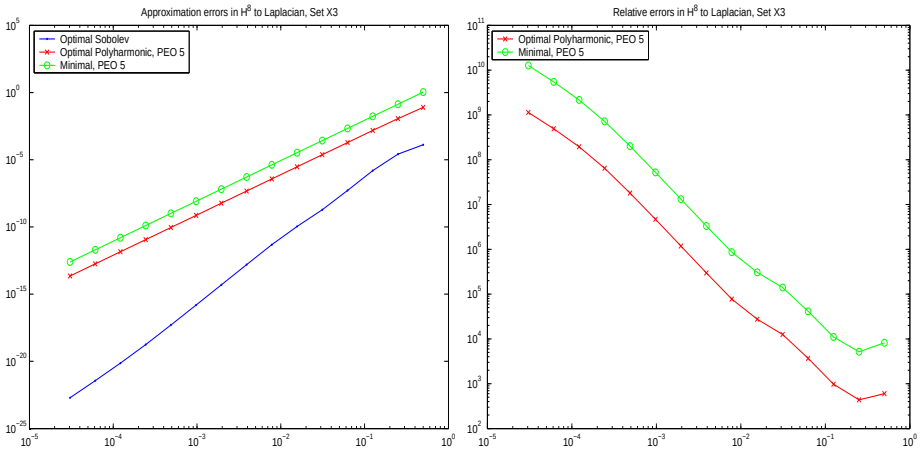
Approximation errors in H^8 to Laplacian, Set X3
Optimal Sobolev
Optimal Polyharmonic, PEO 5
Minimal, PEO 5
Relative errors in H^8 to Laplacian, Set X3
Optimal Polyharmonic, PEO 5
Minimal, PEO 5

Figure 10: Absolute and Sobolev-relative error norms in $W_2^8(\mathbb{R}^2)$ for polyharmonic and minimal approximation of order 5 on set $X3$

[14] N. Flyer, B. Fornberg, V. Bayona, and G.A. Barnett. On the role of polynomials in RBF-FD approximations: I. Interpolation and accuracy. *Journal of Computational Physics*, 321:21–38, 2016.

[15] N. Flyer, E. Lehto, S. Blaise, G.B. Wright, and A. St.-Cyr. A guide to RBF-generated finite differences for nonlinear transport: shallow water simulations on a sphere. preprint, 2015.

[16] S. Gerace, K. Erhart, E. Divo, and A. Kassab. Local and virtual RBF meshless method for high-speed flows. In *Mesh reduction methods—BEM/MRM XXXI*, volume 49 of *WIT Trans. Model. Simul.*, pages 83–94. WIT Press, Southampton, 2009.

[17] T.-T. Hoang-Trieu, N. Mai-Duy, and T. Tran-Cong. Several compact local stencils based on integrated RBFs for fourth-order ODEs and PDEs. *CMES Comput. Model. Eng. Sci.*, 84(2):171–203, 2012.

[18] R. Hosseini, B. Hashemi. Solution of Burgers' equation using a local-RBF meshless method. *Int. J. Comput. Methods Eng. Sci. Mech.*, 12(1):44–58, 2011.

[19] A. Iske. Reconstruction of functions from generalized Hermite-Birkhoff data. In C.K. Chui and L.L. Schumaker, editors, *Approximation Theory VIII, Vol. 1*, pages 257–264. World Scientific, Singapore, 1995.

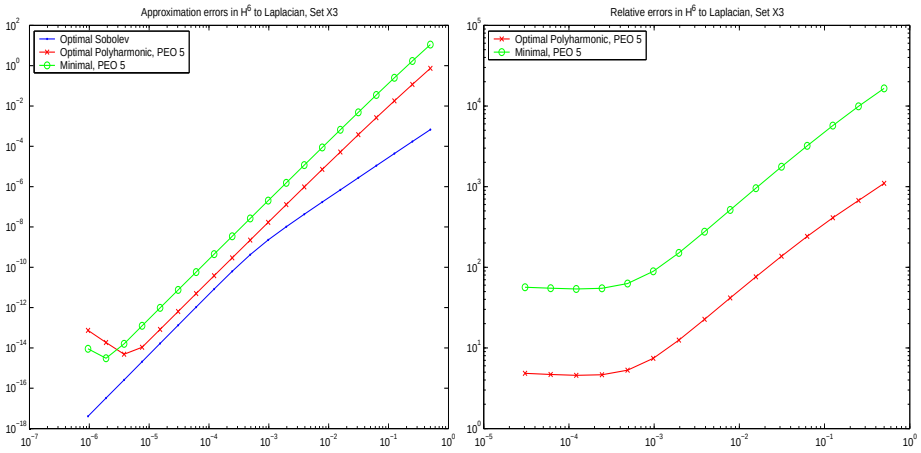
Approximation errors in H^6 to Laplacian, Set X3
Optimal Sobolev
Optimal Polyharmonic, PEO 5
Minimal, PEO 5
Relative errors in H^6 to Laplacian, Set X3
Optimal Polyharmonic, PEO 5
Minimal, PEO 5

Figure 11: Absolute and Sobolev-relative error norms in $W_2^6(\mathbb{R}^2)$ for polyharmonic and minimal approximation of order 5 on set $X3$

[20] A. Iske. On the approximation order and numerical stability of local Lagrange interpolation by polyharmonic splines. In *Modern Developments in Multivariate Approximation*, pages 153–165. Birkhäuser, Basel, 2003.

[21] A. Iske. On the stability of polyharmonic spline reconstruction. In *Conference Proceedings of Sampling Theory and Applications (SampTA2011)*, 2011.

[22] A. Iske. On the construction of kernel-based adaptive particle methods in numerical flow simulation. In R. Ansorge, H. Bijl, A. Meister, and Th. Sonar, editors, *Recent Developments in the Numerics of Nonlinear Hyperbolic Conservation*, Notes on Numerical Fluid Mechanics and Multidisciplinary Design (NNFM), pages 197–221. Springer-Verlag, Berlin, 2013.

[23] E. Kansa. Radial basis functions: achievements and challenges. In *Boundary Elements and Other Mesh Reduction Methods XXXVII*, volume 61 of *WIT Transactions on Modelling and Simulation*, pages xxx–yyy, 2015.

[24] E. Larsson, E. Lehto, A. Heryodono, and B. Fornberg. Stable computation of differentiation matrices and scattered node stencils based on Gaussian radial basis functions. *SIAM J. Sci. Comput.*, 35:A2096–A2119, 2013.

[25] NIST. Digital Library of Mathematical Functions. Technical report, National Institute of Standards and Technology USA, http://dlmf.nist.gov/, 2015.

[26] B. Šarler. From global to local radial basis function collocation method for transport phenomena. In *Advances in meshfree techniques*, volume 5 of *Comput. Methods Appl. Sci.*, pages 257–282. Springer, Dordrecht, 2007.

[27] R. Schaback. Reconstruction of multivariate functions from scattered data. Manuscript, available via http://www.num.math.uni-goettingen.de/schaback/research/group.html, 1997.

[28] R. Schaback. Improved error bounds for scattered data interpolation by radial basis functions. *Mathematics of Computation*, 68:201–216, 1999.

[29] R. Schaback. Multivariate interpolation by polynomials and radial basis functions. *Constructive Approximation*, 21:293–317, 2005.

[30] R. Schaback. Error analysis of nodal meshless methods. preprint, available via the homepage of the author, 2016.

[31] R. Schaback. Superconvergence of kernel-based interpolation. preprint, available via the homepage of the author, 2016.

[32] V. Shankar, G.B. Wright, R.M. Kirby, and A.L. Fogelson. A radial basis function (RBF)-finite difference (FD) method for diffusion and reaction-diffusion equations on surfaces. *J. Sci. Comput.*, 63:745–768, 2015.

[33] C. Shu, H. Ding, and K.S. Yeo. Local radial basis function-based differential quadrature method and its application to solve two-dimensional incompressible Navier-Stokes equations. *Comput. Methods Appl. Mech. Eng.*, 192:941–954, 2003.

[34] C. Shu, H. Ding, and K.S. Yeo. Computation of incompressible Navier-Stokes equations by local RBF-based differential quadrature method. *CMES Comput. Model. Eng. Sci.*, 7(2):195–205, 2005.

[35] D. Stevens, H. Power, M. Lees, and H. Morvan. A local Hermitian RBF meshless numerical method for the solution of multi-zone problems. *Numer. Methods Partial Differential Equations*, 27(5):1201–1230, 2011.

[36] N. Thai-Quang, K. Le-Cao, N. Mai-Duy, and T. Tran-Cong. A high-order compact local integrated-RBF scheme for steady-state incompressible viscous flows in the primitive variables. *CMES Comput. Model. Eng. Sci.*, 84(6):528–557, 2012.

[37] A.I. Tolstykh. On using RBF-based differencing formulas for unstructured and mixed structured-unstructured grid calculations. In *Proceedings of the 16th IMACS World Congress 228*, pages 4606–4624. ISBN 3-9522075-1-9, CD-ROM, 2000.

[38] R. Vertnik and B. Šarler. Local collocation approach for solving turbulent combined forced and natural convection problems. *Adv. Appl. Math. Mech.*, 3(3):259–279, 2011.

[39] H. Wendland. *Scattered Data Approximation*. Cambridge University Press, 2005.

[40] G.B. Wright and B. Fornberg. Scattered node compact finite difference-type formulas generated from radial basis functions. *J. Comput. Phys.*, 212(1):99–123, 2006.

[41] G.M. Yao, B. Šarler, and C. S. Chen. A comparison of three explicit local meshless methods using radial basis functions. *Eng. Anal. Bound. Elem.*, 35(3):600–609, 2011.

[42] G.M. Yao, Siraj ul Islam, and B. Šarler. Assessment of global and local meshless methods based on collocation with radial basis functions for parabolic partial differential equations in three dimensions. *Eng. Anal. Bound. Elem.*, 36(11):1640–1648, 2012.